

# IRSF SIRIUS $JHK_s$ Simultaneous Transit Photometry of GJ1214b

Norio NARITA,<sup>1,7</sup> Takahiro NAGAYAMA,<sup>2</sup> Takuya SUENAGA,<sup>3</sup> Akihiko FUKUI,<sup>4</sup>  
Masahiro IKOMA,<sup>5</sup> Yasushi NAKAJIMA,<sup>1,6</sup> Shogo NISHIYAMA,<sup>1</sup> and Motohide TAMURA<sup>1</sup>

<sup>1</sup> National Astronomical Observatory of Japan, 2-21-1 Osawa, Mitaka, Tokyo, 181-8588, Japan

<sup>2</sup> Department of Astrophysics, Nagoya University, Furo-cho, Chikusa-ku, Nagoya, 464-8602, Japan

<sup>3</sup> Department of Astronomy, Graduate University for Advanced Studies, 2-21-1 Osawa, Mitaka, Tokyo 181-8588, Japan

<sup>4</sup> Okayama Astrophysical Observatory, National Astronomical Observatory of Japan,  
3037-5 Honjo, Kamogata, Asakuchi, Okayama 719-0232, Japan

<sup>5</sup> Department of Earth and Planetary Science, The University of Tokyo, 7-3-1 Hongo, Bunkyo-ku, Tokyo, 113-0033, Japan

<sup>6</sup> Hitotsubashi University 2-1, Naka, Kunitachi, Tokyo, Japan, 186-8601

<sup>7</sup> NAOJ Fellow

norio.narita@nao.ac.jp

(Received 2012 August 9; accepted 2012 October 11)

## Abstract

We report high precision transit photometry of GJ1214b in  $JHK_s$  bands taken simultaneously with the SIRIUS camera on the IRSF 1.4 m telescope at Sutherland, South Africa. Our MCMC analyses show that the observed planet-to-star radius ratios in  $JHK_s$  bands are  $R_p/R_{s,J} = 0.11833 \pm 0.00077$ ,  $R_p/R_{s,H} = 0.11522 \pm 0.00079$ ,  $R_p/R_{s,K_s} = 0.11459 \pm 0.00099$ , respectively. The radius ratios are well consistent with the previous studies by Bean et al. (2011) within  $1\sigma$ , while our result in  $K_s$  band is shallower than and inconsistent at  $4\sigma$  level with the previous measurements in the same band by Croll et al. (2011). We have no good explanation for this discrepancy at this point. Our overall results support a flat transmission spectrum in the observed bands, which can be explained by a water-dominated atmosphere or an atmosphere with extensive high-altitude clouds or haze. To solve the discrepancy of the radius ratios and to discriminate a definitive atmosphere model for GJ1214b in the future, further transit observations around  $K_s$  band would be especially important.

**Key words:** stars: planetary systems: individual (GJ1214) — techniques: photometric

## 1. Introduction

Among several hundreds of discovered extrasolar planets, transiting exoplanets can give us the most information about properties of planets. Transiting exoplanets are unique in that both the true mass and the radius can be determined by measurements of radial velocities and transit depths. The mass-radius relation enables us to infer the internal structure and bulk compositions of transiting exoplanets (e.g., Valencia et al. 2007). One can also measure the angle between the stellar spin axis and the planetary orbital axis in the sky projection via the Rossiter-McLaughlin effect, which provides insights of planetary migration histories (e.g., Winn et al. 2005; Narita et al. 2007; Hébrard et al. 2008; Narita et al. 2009; Winn et al. 2009; Triaud 2011; Hirano et al. 2011; Albrecht et al. 2012). Another great merit of transiting planets is that they also provide opportunities to probe atmospheric compositions by transit photometry or spectroscopy. Theoretical predictions have shown that transit depths depend on wavelengths (e.g., Seager & Sasselov 2000; Miller-Ricci & Fortney 2010; Howe & Burrows 2012), reflecting atmospheric compositions and environments (e.g., haze/clouds). Previous space-based and ground-based observations for transiting hot Jupiters have indeed revealed that this methodology, often referred

to as transmission spectroscopy, is useful to learn exoplanetary atmospheres (e.g., Charbonneau et al. 2002; Winn et al. 2004; Narita et al. 2005; Redfield et al. 2008; Snellen et al. 2008; Swain et al. 2008; Désert et al. 2009; Sing et al. 2011).

Recent discoveries of transiting planets with smaller radii (i.e., a few Earth radii) around M dwarfs have expanded targets of this methodology down to terrestrial exoplanets. Transiting planets around M dwarfs are especially favorable for this kind of studies since transit depths become relatively deeper due to smaller host stars' radii. In this sense, GJ1214b discovered by Charbonneau et al. (2009) is currently the most interesting target. Numbers of previous observers reported transit depths of GJ1214b in various wavelength bands (e.g., Bean et al. 2010; Bean et al. 2011; Croll et al. 2011; Désert et al. 2011; Carter et al. 2011; Berta et al. 2011; Berta et al. 2012; de Mooij et al. 2012). The previous observations have revealed that there are two possible atmospheric models to explain the observed transit depths: a water-dominated (higher mean molecular weight / lower scale height) atmosphere and a hydrogen-dominated (lower mean molecular weight / higher scale height) atmosphere. Among the previous studies, supporting evidences for the hydrogen-dominated atmosphere are deeper transit depths observed in  $K_s$  band (Croll et al. 2011; de Mooij et al. 2012) and in g band (de

Mooij et al. 2012). The rest of observations have shown a fairly flat transmission spectrum for GJ1214b through visible and infrared wavelengths, which indicates the water-dominated atmosphere or the hydrogen-dominated but with high-altitude clouds/haze atmosphere. Thus the nature of this planetary atmosphere is still an open question.

One known problem of GJ1214 as a target of transit photometry is possible stellar variability and starspots, which may cause small time-dependent variations in transit depths. Some of the previous studies estimated that such small variations would correspond to the ratio of radii of the planet and star  $R_p/R_s \sim 0.001$  (Carter et al. 2011; Berta et al. 2011; de Mooij et al. 2012), which are indeed comparable to or larger than the nominal observational uncertainties reported in the previous publications. This fact makes it difficult to compare the all observed transit depths in different epochs. For this reason, simultaneous multi-band transit photometry is the most useful way to discriminate possible atmosphere models. We thus focus on JHK<sub>s</sub> simultaneous transit photometry since the largest difference in transit depths is theoretically predicted between JH bands and K<sub>s</sub> band. In this sense, our motivation is the same as that by Croll et al. (2011), who tried nearly simultaneous J and K<sub>s</sub> band transit photometry by rapidly switching the two bandpass filters. Interestingly, Croll et al. (2011) claimed that K<sub>s</sub> band transit depth is significantly ( $5\sigma$ ) deeper than that in J band. With sufficient precision, we can independently confirm or refute the claim by Croll et al. (2011) via JHK<sub>s</sub> simultaneous transit photometry.

In this paper, we present a result of such an observation using the SIRIUS camera onboard the IRSF 1.4 m telescope. This is indeed the first high precision transit observation using IRSF/SIRIUS. We summarize target properties and observation methods in section 2, and describe our analysis methods in section 3. We report our analysis results in section 4, and discuss its meaning in section 5. Finally, we summarize this paper in section 6.

## 2. IRSF SIRIUS Observation for GJ1214

### 2.1. Target Properties

The host star GJ1214 is an M4.5 type star at 13 pc away from the Sun, with a mass of  $0.157 \pm 0.019 M_\odot$  and a radius of  $0.2110 \pm 0.0097 R_\odot$  (The star is known to show stellar variability at  $\sim 2\%$  level with a period of  $\sim 52.3$  d (see e.g., Berta et al. 2011) and also known to have starspots with surface coverage variability at several percent level (Carter et al. 2011).

The orbiting planet GJ1214b is categorized as a super-Earth with a mass of  $6.55 \pm 0.98 M_\oplus$  and a radius of  $2.68 \pm 0.13 R_\oplus$  (Charbonneau et al. 2009). The planet orbits around GJ1214 at a period of  $\sim 1.58$  d and a semi-major axis of  $\sim 0.0146$  AU, where is slightly closer to the host star than the star's habitable zone ( $a_{\text{HZ}} \sim 0.06$  AU). Previous investigation of transit timing variations (TTV) has shown no evidence of large TTV in this system (Carter et al. 2011).

**Table 1.** Photometric transit light curves of GJ1214b taken by IRSF/SIRIUS

Time [BJD <sub>TDB</sub> ]	Value	Error
J band		
2455788.28330	0.99979	0.00124
2455788.28396	1.00011	0.00124
2455788.28462	1.00125	0.00124
2455788.28527	1.00137	0.00125
2455788.28593	1.00015	0.00125

\* All data are presented in the electric table.

### 2.2. Observation Setup

We observed a full transit of GJ1214b during 18:43–21:00 of UT 2011 August 14 with Simultaneous Infrared Imager for Unbiased Survey (SIRIUS: Nagayama et al. 2003) on the Infrared Survey Facility (IRSF) 1.4 m telescope. The IRSF and the SIRIUS camera were constructed and has been operated by Nagoya University, SAAO (South African Astronomical Observatory) at Sutherland, South Africa, and National Astronomical Observatory of Japan. The SIRIUS camera utilizes two dichroic filters and three  $1024 \times 1024$  HgCdTe detectors, which can obtain J ( $1.25\mu\text{m} \pm 0.085\mu\text{m}$ ), H ( $1.63\mu\text{m} \pm 0.15\mu\text{m}$ ), K<sub>s</sub> ( $2.14\mu\text{m} \pm 0.16\mu\text{m}$ ) band images simultaneously, with a square field of view of  $7.7'$  on a side and a pixel scale of  $0.45''$ . To achieve higher photometric precision, we defocused the telescope so that stars have doughnut-like point spread function (PSF). The typical size of the PSF was  $\sim 13$  pixels in radius. We carefully set GJ1214 and bright comparison stars away from bad pixels on the detectors. The exposure time was 49 s and the typical dead time was 7.6 s (duty cycle of 86.6%). As a result, we obtained 145 frames during the above time and use them for subsequent analyses.

### 2.3. Position-Locking Software

For high precision infrared photometry, it is known that target positions on the detectors should be stared rather than dithered (see e.g., Croll et al. 2011). Since the IRSF does not equip an auto-guider, target positions tend to move over tens of pixels during observations and it was the biggest problem for precise transit observations with the IRSF. To avoid such changes of target positions, we have developed and installed a customized position-locking software which gives appropriate feedback to the telescope when the centroid position of the target star moves over 1 pixel on the detectors. By using the position-locking software, GJ1214's centroid positions on the three detectors are kept within an rms of about 2 pixels in both x and y directions.

## 3. Data Reduction and Light Curve Analysis

Primary data reduction is carried out with a pipeline for the SIRIUS<sup>1</sup>, including a correction for non-linearity,

<sup>1</sup> <http://www.z.phys.nagoya-u.ac.jp/~nakajima/sirius/software/software.html>

dark subtraction, and flat fielding. We note that the detectors of SIRIUS saturate at 32000 ADU (J band detector), 33000 ADU (H band detector), and 25000 ADU (K<sub>s</sub> band detector) respectively under the Correlated Double-Sampling (CDS) readout mode, and keep a good linearity ( $\leq 1\%$ ) up to  $\sim 10000$  ADU. The above non-linearity correction enables us to work up to  $\sim 25000$  ADU with  $\leq 1\%$  linearity. The correction is necessary to reduce possible systematic errors stemmed from non-linearity in fractional light curves down to  $\leq 0.1\%$ . This is especially important for H and K<sub>s</sub> bands where sky background levels are high.

Aperture photometry is followed using a customized aperture photometry pipeline (Fukui et al. 2011), with a constant aperture-size mode where a same aperture size is applied for all images. Sky background levels on the observing night were typically  $\sim 1000$  ADU,  $\sim 7000$  ADU, and  $\sim 6000$  ADU, for JHK<sub>s</sub> bands, respectively. Maximum counts in the frames (including sky background) are below 25000 ADU, where the non-linearity correction can work.

Time stamps of observations are recorded in the FITS headers in units of Modified Julian Day (MJD) based on Coordinated Universal Time (UTC). We convert the time system to Barycentric Julian Day (BJD) based on Barycentric Dynamical Time (TDB) using the code by Eastman et al. (2010).

We then select appropriate comparison stars and aperture radii for each band so that light curves have the smallest rms at out-of-transit (OOT) phase as follows. There are three possible comparison stars within the field of view of SIRIUS: one is almost the same brightness as GJ1214 and the others are 1-2 magnitude fainter than GJ1214. First, we create fractional light curves by dividing fluxes of GJ1214 by sum of all combinations of comparison stars' fluxes with changing the aperture radius from 13 pixels to 30 pixels in increments of 1 pixel. All the fractional light curves  $F_{\text{obs}}$  exhibit systematic trends (0.1% level and apparently linear) at OOT phase. The systematic trends could arise due to slow variability in the brightness of GJ1214 itself or comparison stars, changing airmass, or position changes of the stars on the detectors, and so on. We then correct the systematic trends by the following expression,  $F_{\text{cor}} = F_{\text{obs}} \times 10^{-0.4\Delta m_{\text{cor}}}$ , by assuming the correction factor  $\Delta m_{\text{cor}} = k_0 + k_t t + k_z z + k_x dx + k_y dy$ , where  $t$  is the time,  $z$  is the airmass,  $dx$  and  $dy$  are the differences of centroid positions in x and y directions, and  $k_0, k_t, k_z, k_x, k_y$  are free coefficients. We eliminate outliers (2, 10, 1 frames for JHK<sub>s</sub> bands, respectively) with large centroid position changes over 10 pixels, and determine optimal coefficients using OOT data by the AMOEBA algorithm (Press et al. 1992) so that the corrected OOT data have the smallest rms. In this process, we also rescale the photometric errors of the data so that reduced  $\chi^2$  become unity. We consequently choose to use only the brightest comparison star (the same one for all bands) and aperture radii of 15, 16, 15 pixels for JHK<sub>s</sub> bands, which give the smallest rms of the data as 0.00124, 0.00125, 0.00155 for JHK<sub>s</sub> bands, respectively. We note that including the other two comparison stars or using different aperture radii have less impact on our subsequent conclusion,

but with slightly larger errors. The data of the corrected transit light curves are presented in table 1.

For modeling the corrected transit light curves, we follow the procedures that were adopted in previous studies in literature (Bean et al. 2011; Croll et al. 2011; de Mooij et al. 2012; Berta et al. 2012) so as to compare our transit depths with previous ones. We fix the orbital inclination  $i$  to  $88.94^\circ$  and the orbital distance in units of the stellar radius  $a/R_s$  to 14.9749, which were determined by Bean et al. (2010). We also fix the orbital period of GJ1214b ( $P = 1.58040481$  d) and the mid-transit time ( $T_{c,0} = 2454966.525123$  BJD<sub>TDB</sub>), determined by Bean et al. (2011). This assumption is justified by the fact that there is no evidence of large TTV (Carter et al. 2011). We use the quadratic limb-darkening law,  $I(\mu) = 1 - u_1(1 - \mu) - u_2(1 - \mu)^2$ , where  $I$  is the intensity and  $\mu$  is the cosine of the angle between the line of sight and the line from the stellar center to the position of the stellar surface. We adopt empirical quadratic limb-darkening coefficients ( $u_{1,J} = 0.088$ ,  $u_{2,J} = 0.404$ ,  $u_{1,H} = 0.076$ ,  $u_{2,H} = 0.407$ ,  $u_{1,K_s} = 0.048$ ,  $u_{2,K_s} = 0.350$ ) for JHK<sub>s</sub> bands given by Claret & Bloemen (2011), assuming stellar effective temperature  $T_{\text{eff}} = 3000$  K and log of the stellar surface gravity  $\log g = 5.0$ . We note that these assumptions on  $T_{\text{eff}}$  and  $\log g$  are the same as Croll et al. (2011) for J and K<sub>s</sub> bands, although Croll et al. (2011) used the non-linear limb-darkening law.

We fit the JHK<sub>s</sub> transit light curves simultaneously using the analytic formula given by Ohta et al. (2009), which is equivalent with Mandel & Agol (2002) when using the quadratic limb-darkening law. The four free parameters are the difference of the observed mid-transit time from the predicted mid-transit time  $\Delta T_c$  for this epoch (epoch  $E = 520$  from  $T_{c,0}$ ) and the radius ratios of the planet and star  $R_p/R_s$  for JHK<sub>s</sub> bands. In addition to the main analysis, we also test some other cases with different conditions as follows: (1)  $T_c$  for each band to be free, (2)  $u_2$  for each band to be free, and (3)  $i$  and  $a/R_s$  to be free, to assess the validness of assumptions of fixed parameters above. We employ the Markov Chain Monte Carlo (MCMC) method to estimate values and uncertainties of the free parameters, following the analysis by Croll et al. (2011). We create 5 chains of 5,000,000 points, then trim the first 100,000 points from each chain. The acceptance ratios of jumping for the chains are set to about 25%, and we check that they pass the Gelman & Rubin (1992) test. We define  $1\sigma$  statistical errors by the range of parameters between 15.87% and 84.13% of merged posterior distributions.

#### 4. Results

The mean values and  $1\sigma$  statistical errors based on the MCMC analyses are summarized in table 2. We note that the errors do not include systematic errors discussed in the next section. In the main analysis, we find  $\Delta T_c = 0.000104 \pm 0.000067$  s, which is consistent with the predicted mid-transit time within  $2\sigma$ , validating the assumption to use the fixed period determined

**Table 2.** Mean values and errors of the parameters based on the MCMC analyses.

Parameter	Value	Error <sup>†</sup>	Value	Error	Value	Error	Value	Error
	main		case (1)		case (2)		case (3)	
$R_p/R_{s,J}$	0.11833	$\pm 0.00077$	0.11833	$\pm 0.00077$	0.11867	$\pm 0.00095$	0.11800	$\pm 0.00083$
$R_p/R_{s,H}$	0.11522	$\pm 0.00079$	0.11519	$\pm 0.00079$	0.11668	$\pm 0.00096$	0.11492	$\pm 0.00085$
$R_p/R_{s,K_s}$	0.11459	$\pm 0.00099$	0.11463	$\pm 0.00099$	0.11428	$\pm 0.00121$	0.11427	$\pm 0.00101$
$\Delta T_{c,all}$ [s]	0.000104	$\pm 0.000067$	–	–	0.000107	$\pm 0.000066$	0.000102	$\pm 0.000069$
$\Delta T_{c,J}$ [s]	–	–	0.000111	$\pm 0.000111$	–	–	–	–
$\Delta T_{c,H}$ [s]	–	–	0.000005	$\pm 0.000114$	–	–	–	–
$\Delta T_{c,K_s}$ [s]	–	–	0.000244	$\pm 0.000134$	–	–	–	–
$u_{2,J}$	0.404	fixed	0.404	fixed	0.345	$\pm 0.095$	0.404	fixed
$u_{2,H}$	0.407	fixed	0.407	fixed	0.145	$\pm 0.103$	0.407	fixed
$u_{2,K_s}$	0.350	fixed	0.350	fixed	0.403	$\pm 0.125$	0.350	fixed
$i$ [°]	88.94	fixed	88.94	fixed	88.94	fixed	89.13	$+0.53$ $-0.44$
$a/R_s$	14.9749	fixed	14.9749	fixed	14.9749	fixed	15.0468	$+0.3413$ $-0.4847$

<sup>†</sup> The presented errors do not include systematic errors due to the fixed parameters (see text).

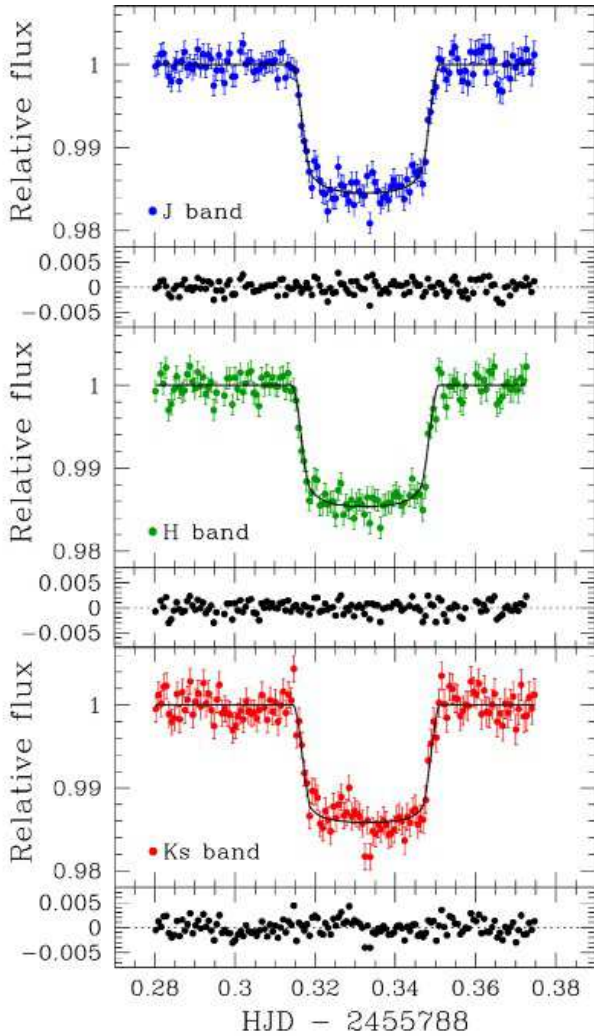


**Fig. 1.** Transit light curves with the best-fit models in J (top panel), H (middle panel),  $K_s$  (bottom panel) bands, observed simultaneously by the IRSF/SIRIUS. Each lower panel shows residuals between the observed values and the best-fit models.

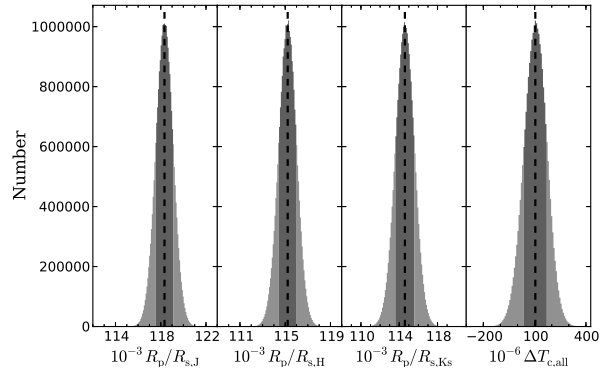


**Fig. 2.** MCMC histograms of the free parameters. The binning size is set to a hundredth part of the plotting region. The dashed vertical line in each panel indicates the mean value. The thick zones represent the  $1\sigma$  statistical errors shown in table 2.

by Bean et al. (2011). The derived radius ratios are  $R_p/R_{s,J} = 0.11833 \pm 0.00077$ ,  $R_p/R_{s,H} = 0.11522 \pm 0.00079$ ,  $R_p/R_{s,K_s} = 0.11459 \pm 0.00099$ , respectively. Comparisons of our result with the previous studies are discussed in the next section. Figure 1 plots the transit light curves with the models using the mean MCMC values, and figure 2 shows histograms of the posterior distribution of the free parameters.

One may wonder why our errors are comparable with Croll et al. (2011), even though we observed only one transit with the IRSF 1.4m telescope and Croll et al. (2011) observed 3 transits with the CFHT 3.8m telescope. The reasons are that Croll et al. (2011) switched between J and  $K_s$  band filters during the transits and the 3.8m telescope was too large for the brightness of GJ1214. Namely, Croll et al. (2011) employed 4 s exposure and the total duty cycle was only 22% for J and  $K_s$  bands, which is significantly lower than our duty cycle of 86.6%. Considering the above fact, it is reasonable that our errors are similar to those by Croll et al. (2011).

From the case (1), we find that  $\Delta T_c$  for JHK<sub>s</sub> bands are all consistent with zero within  $2\sigma$  and one another. Also, the result shows that fitting  $\Delta T_c$  for JHK<sub>s</sub> bands at once or separately has less impact on radius ratios.

The case (2) illustrates a potential of systematic errors and underestimated errors stemmed from the fixed limb-darkening coefficients. The derived  $u_2$  for J and K<sub>s</sub> bands are well consistent with the empirical values by Claret & Bloemen (2011), and then the radius ratios in the same bands are also well accorded with the main result. While the derived  $u_2$  in H band is  $\sim 2.5\sigma$  apart from the empirical value, and the radius ratio is also different from the main result by  $\sim 1.5\sigma$ . Although some systematic errors may be present, we consider that the assumption of the adopted limb-darkening coefficients is reasonable for the mean values, since the empirical values are in excellent agreement with the derived values in J and K<sub>s</sub> bands. For this reason, we believe that the radius ratio in H band using the empirical limb-darkening coefficients (the main case) is more reliable than that with free  $u_2$  (the case 2). Another fact seen from the case (2) is that the errors of the radius ratios are about 20% larger than the main case where the limb-darkening coefficients are fixed. This fact is often pointed out in previous studies (e.g., Southworth 2008). Thus we note that the quoted errors in the radius ratios with the fixed limb-darkening coefficients may have 20% additional errors.

Finally, we confirm that the orbital inclination ( $i$ ) and the orbital distance in units of the stellar radius ( $a/R_s$ ) derived from our IRSF data are well consistent with those by Bean et al. (2010) via the analysis of case (3). We also confirm the derived radius ratios are consistent with the main result, however we notice that the errors are about 10% larger than the main result. This fact also suggests that errors may be about 10% underestimated when using the fixed  $i$  and  $a/R_s$ .

## 5. Discussions

### 5.1. Impacts of Systematic Errors

In this section, we compare our radius ratios in JHK<sub>s</sub> bands with the previous studies and atmospheric models. Before doing that, we should care about possible systematic errors.

First, as assessed by the test cases (2) and (3), we note that our statistical errors may have additional 30% uncertainties due to the systematic errors stemmed from the fixed parameters (20% from fixing the limb-darkening coefficients, and 10% from fixing the orbital inclination and the orbital distance).

Second, it is also necessary to consider impacts of stellar flux variability and stellar spots on our results so as to compare radius ratios with previous studies measured in different epochs and wavelengths. Désert et al. (2011) presented an equation for estimating a difference of radius ratio  $\Delta(R_p/R_s)$  caused by stellar flux variability due to unocculted spots (see equation 7 of Désert et al. 2011). The equation can be rewritten as

$$\Delta(R_p/R_s) \simeq 0.5 \Delta f(\lambda) (R_p/R_s), \quad (1)$$

where  $\Delta f(\lambda)$  is stellar flux variability at wavelength  $\lambda$ . Berta et al. (2011) reported stellar flux variability of  $\sim 2\%$  level in the MEarth observing bandpass ( $\sim 780\text{nm}$ ), and if following the assumption used in Croll et al. (2011) that GJ1214 ( $T_{\text{eff}} \sim 3000\text{K}$ ) has spots 500 K cooler, then the stellar flux variabilities in JHK<sub>s</sub> bands can translate into  $\sim 1.5\%$ ,  $\sim 1.3\%$ ,  $\sim 1.0\%$ , respectively (Croll et al. 2011). Using the equation above, possible variability of radius ratios in JHK<sub>s</sub> bands are  $\sim 0.75\%$ ,  $\sim 0.65\%$ ,  $\sim 0.5\%$  of the observed radius ratios. Thus we should take into account possible systematic differences of  $\Delta(R_p/R_{s,J}) \sim 0.00089$ ,  $\Delta(R_p/R_{s,H}) \sim 0.00075$ ,  $\Delta(R_p/R_{s,K_s}) \sim 0.00057$ , when comparing our radius ratios with other epochs' results.

Third, although we do not find any clear sign of spot occultation in our data, possible existence of unocculted spots is still a problem when comparing radius ratios with theoretical atmospheric models, since their impact depends not only on wavelength but also on spot properties (coverage, temperature, and so on) and GJ1214's spot properties are still unclear. de Mooij et al. (2012) presented corrections for radius ratios assuming several cases of different spot coverage. According to their study, the corrections vary greatly between optical and infrared wavelength ( $\Delta(R_p/R_s) \sim 0.003$  if spot coverage is 5%), but corrections in JHK<sub>s</sub> bands are very similar (see figure 7 of de Mooij et al. 2012). Thus we neglect the corrections for the current study since our data are only in JHK<sub>s</sub> bands, although we should take care when comparing our radius ratios with those in optical bands.

### 5.2. Comparisons with the Previous Studies

Figure 3 plots our observed radius ratios with those in the previous studies (Bean et al. 2011; Croll et al. 2011; Désert et al. 2011; Berta et al. 2012; de Mooij et al. 2012) and the two atmospheric models (i.e., hydrogen-dominated and water-dominated atmospheres) by Miller-Ricci & Fortney (2010). Note that the values and errors of the previous studies are reported ones without any corrections, and the errors of our data are based on the MCMC analysis (30% additional errors are not included, since previous observers did not take into account such systematic errors).

In summary, our results support a featureless transmission spectrum with a shallower (without a deeper) transit in K<sub>s</sub> band, which favors a water-dominated atmosphere rather than a cloudless hydrogen-dominated atmosphere by Miller-Ricci & Fortney (2010). A similar flat transmission spectrum can be expected if the atmosphere is covered by optically thick high-altitude clouds or haze (see e.g., Bean et al. 2011; Berta et al. 2012).

A similar conclusion was also reported by Bean et al. (2011), who observed two transits of GJ1214b using the MMIRS instrument of the Magellan telescope by the multi-object spectroscopy approach. They obtained radius ratios of GJ1214b in JHK bands (almost the same bandpass with our bands) as  $R_p/R_{s,J} = 0.1158 \pm 0.0024$ ,

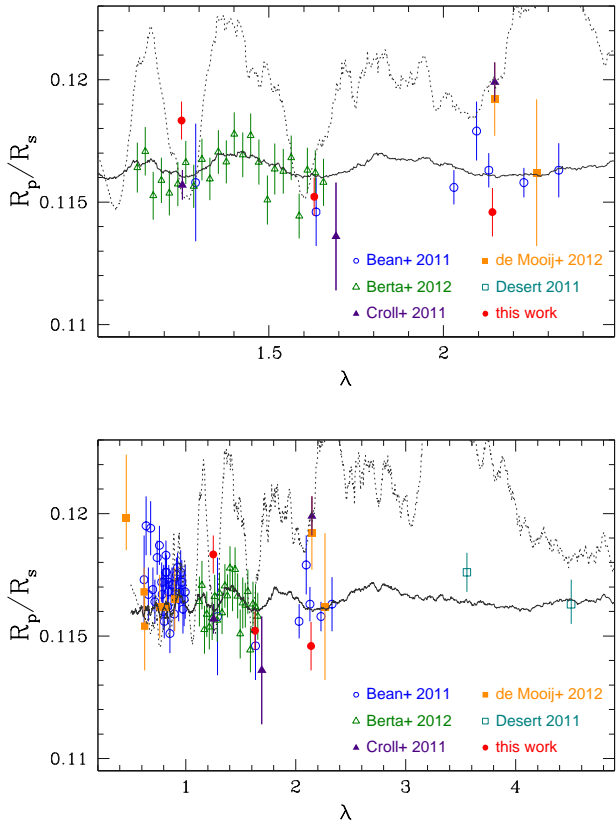


**Fig. 3.** Comparisons of our results with the previous observational studies and the cloudless atmospheric models by Miller-Ricci & Fortney (2010). The gray solid line represents the water-dominated (vapor) atmosphere model, and the gray dotted line does the hydrogen-dominated (Solar composition) model. The upper figure shows 1-2.5  $\mu\text{m}$  wavelength region and the lower one does 0.6-4.5  $\mu\text{m}$  region.

$R_p/R_{s,H} = 0.1146 \pm 0.0014$ ,  $R_p/R_{s,K} = 0.1158 \pm 0.0006$ , respectively. Thus our radius ratios in JHK<sub>s</sub> bands are all consistent with Bean et al. (2011) within a square-root of sum of squares of both  $1\sigma$  errors. Our radius ratios in J and H bands are also in agreement with Berta et al. (2012), who conducted spectro-photometry in the band-pass between 1.1 and 1.7  $\mu\text{m}$  using the Wide Field Camera 3 (WFC3) onboard the Hubble Space Telescope.

On the other hand, our radius ratio in K<sub>s</sub> band appears inconsistent with the previous measurements in the same band by Croll et al. (2011) ( $R_p/R_{s,K_s} = 0.1199 \pm 0.0008$ ) and de Mooij et al. (2012) ( $R_p/R_{s,K_s} = 0.1189 \pm 0.0015$ ). Especially, our result ( $R_p/R_{s,K_s} = 0.1146 \pm 0.0010$ ) differs about  $4\sigma$  ( $1\sigma$  here is a square-root of sum of squares of both  $1\sigma$  errors) from that by Croll et al. (2011). The discrepancy cannot be explained by stellar flux variability in K<sub>s</sub> band ( $\Delta(R_p/R_{s,K_s}) \sim 0.00057$ ) nor 30% additional systematic errors due to the fixed parameters. Thus we do not confirm a deeper transit in K<sub>s</sub> band and we have no clear explanation for this discrepancy at this point in time. Further transit observations in K<sub>s</sub> band would be necessary to solve this enigma.

### 5.3. Possible Origins of Water-Dominated Atmospheres

The investigation of planetary atmospheres provides a crucial clue to learn the bulk composition of super-Earths like GJ1214b, which also gives important constraints on formation processes of such planets. Only with its measured mass and radius, we are unable to distinguish whether GJ1214b is a rocky planet with a thick H/He atmosphere or a water-dominated atmosphere (Rogers & Seager 2010; Nettelmann et al. 2011). Transmission spectroscopy is thus an important key to discriminate the atmospheric nature of transiting planets. As discussed earlier, our finding as well as some of the previous studies (e.g., Bean et al. 2011; Désert et al. 2011; Berta et al. 2012) support a possibility of a water-dominated atmosphere for GJ1214b. Then, how can such atmospheres form?

According to detailed modeling of the internal structure by Nettelmann et al. (2011), however, two-layer models (a water envelope on top of a rock core) which are consistent with GJ1214's age would have unreasonably high water-to-rock ratio. To fix this problem, a small amount of H/He, which accounts for several percent of the planet's total mass, must be incorporated in the water envelope (see Figure 4 of Nettelmann et al. 2011). In other words, GJ1214b is a Uranus/Neptune-like planet whose atmosphere is heavily polluted by water.

Such properties of GJ1214b are qualitatively consistent with recent theories of planet formation. GJ1214b is orbiting close to its host star, in contrast to Uranus and Neptune. Its current location was too hot for icy building blocks to exist in the proto-planetary disk where the planet was born. Therefore, provided GJ1214b contains a significant amount of water, it is reasonable to think that the planet has experienced orbital migration.

One possible mechanism for migration is angular-momentum exchange with the proto-planetary disk (i.e., the type-I migration; Ward 1986). Recent  $N$ -body simulations of planetary accretion with the effect of the type-I migration have demonstrated that water-rich proto-planets of super-Earth-size can form in the vicinity of the central star (Ogihara & Ida 2009). As the proto-planets are embedded in the disk, they also capture the ambient H/He disk gas naturally. A proto-planet with mass similar to that of GJ1214b can gain H/He atmosphere comparable in mass with that predicted by Nettelmann et al. (2011), although it depends on values of several parameters (Ikoma & Hori 2012). Then, bombardments of smaller planetary embryos and/or other proto-planets rich in water can heavily pollute the H/He atmosphere by water during and after the migration.

Another possibility is that a Uranus/Neptune-like planet that had formed beyond the snow line has migrated by gravitational scattering or by long-term interaction with outer gravitationally perturbing objects. Beyond the snow line, icy planetesimals are sufficiently available for polluting H/He atmospheres. Indeed, the metallicity of the atmospheres of Uranus and Neptune are known to be significantly super-solar (Hubbard et al. 1995), which sug-

gest such pollutions.

While both scenarios are to be quantitatively verified, the both scenarios suggest that there are other planets yet undetected in the GJ1214b system, although no TTV sign has been found (e.g., Carter et al. 2011). Future search for additional planets with RV measurements (possibly using brighter NIR region) is expected to verify the above scenarios. Moreover, a measurement of the spin-orbit alignment angle of GJ1214b via the Rossiter-McLaughlin effect would be very helpful in knowing which of the above two scenarios is true.

## 6. Summary

We conducted high precision JHK<sub>s</sub> simultaneous transit photometry for GJ1214b using the SIRIUS camera on the IRSF at South Africa. It was the first high precision transit observation using IRSF/SIRIUS. In this process, we have demonstrated that high precision NIR transit photometry is possible even without an auto-guider by the position-locking software installed on the telescope. We have found a featureless transmission spectrum in the observed bands, which suggests a water-dominated atmosphere or an atmosphere with extensive high-altitude clouds/haze. Although the observed radius ratios are well consistent with the results by Bean et al. (2011) and Berta et al. (2012), our result in K<sub>s</sub> band is unaccountably inconsistent with the previous studies in the same band by Croll et al. (2011). We have no good explanation for this discrepancy at this point. To solve the discrepancy and to distinguish a definitive atmosphere model for this planet, further transit observations around K<sub>s</sub> band would be especially important. In addition, it will be also interesting to observe transits in blue optical bands in order to ascertain the Rayleigh scattering in the atmosphere of GJ1214b. With such additional observations, we will be able to learn the true nature of the atmosphere of GJ1214b, and discriminating the true atmospheric nature would also give us useful insights on the formation process of this planet.

We acknowledge Eliza Miller-Ricci Kempton for kindly providing their atmospheric models. We thank Eric Gaidos, Teruyuki Hirano, Masayuki Kuzuhara, Hiroshi Ohnuki, and Yasuhiro Takahashi for fruitful discussions. We acknowledge a support by NINS Program for Cross-Disciplinary Study. N.N. is supported by NAOJ Fellowship and by the JSPS Grant-in-Aid for Research Activity Start-up No. 23840046. The IRSF project was financially supported by the Sumitomo foundation and Grants-in-Aid for Scientific Research on Priority Areas (A) (Nos. 10147207 and 10147214) from the Ministry of Education, Culture, Sports, Science and Technology (MEXT). The operation of IRSF is supported by Joint Development Research of National Astronomical Observatory of Japan, and Optical Near-Infrared Astronomy Inter-University Cooperation Program, funded by the MEXT. This work is partly supported by a Grant-in-Aid for Specially Promoted

Research, No. 22000005 from the MEXT and by the Mitsubishi Foundation.

## References

- Albrecht, S., et al. 2012, *ApJ*, 757, 18  
 Bean, J. L., Miller-Ricci Kempton, E., & Homeier, D. 2010, *Nature*, 468, 669  
 Bean, J. L., et al. 2011, *ApJ*, 743, 92  
 Berta, Z. K., Charbonneau, D., Bean, J., Irwin, J., Burke, C. J., Désert, J.-M., Nutzman, P., & Falco, E. E. 2011, *ApJ*, 736, 12  
 Berta, Z. K., et al. 2012, *ApJ*, 747, 35  
 Carter, J. A., Winn, J. N., Holman, M. J., Fabrycky, D., Berta, Z. K., Burke, C. J., & Nutzman, P. 2011, *ApJ*, 730, 82  
 Charbonneau, D., Brown, T. M., Noyes, R. W., & Gilliland, R. L. 2002, *ApJ*, 568, 377  
 Charbonneau, D., et al. 2009, *Nature*, 462, 891  
 Claret, A., & Bloemen, S. 2011, *A&A*, 529, A75  
 Croll, B., Albert, L., Jayawardhana, R., Miller-Ricci Kempton, E., Fortney, J. J., Murray, N., & Neilson, H. 2011, *ApJ*, 736, 78  
 de Mooij, E. J. W., et al. 2012, *A&A*, 538, A46  
 Désert, J.-M., Lecavelier des Etangs, A., Hébrard, G., Sing, D. K., Ehrenreich, D., Ferlet, R., & Vidal-Madjar, A. 2009, *ApJ*, 699, 478  
 Désert, J.-M., et al. 2011, *ApJL*, 731, L40  
 Désert, J.-M., et al. 2011, *A&A*, 526, A12  
 Eastman, J., Siverd, R., & Gaudi, B. S. 2010, *PASP*, 122, 935  
 Fukui, A., et al. 2011, *PASJ*, 63, 287  
 Gelman, A., & Rubin, D. 1992, *Statistical Science*, 7, 457  
 Hébrard, G., et al. 2008, *A&A*, 488, 763  
 Hirano, T., Suto, Y., Winn, J. N., Taruya, A., Narita, N., Albrecht, S., & Sato, B. 2011, *ApJ*, 742, 69  
 Howe, A. R., & Burrows, A. S. 2012, *ApJ*, 756, 176  
 Hubbard, W. B., Podolak, M., & Stevenson, D. J. 1995, in *Neptune and Triton*, ed. D. P. Cruikshank, M. S. Matthews, & A. M. Schumann, 109–138  
 Ikoma, M., & Hori, Y. 2012, *ApJ*, 753, 66  
 Mandel, K., & Agol, E. 2002, *ApJL*, 580, L171  
 Miller-Ricci, E., & Fortney, J. J. 2010, *ApJL*, 716, L74  
 Nagayama, T., et al. 2003, in *Society of Photo-Optical Instrumentation Engineers (SPIE) Conference Series*, Vol. 4841, *Society of Photo-Optical Instrumentation Engineers (SPIE) Conference Series*, ed. M. Iye & A. F. M. Moorwood, 459–464  
 Narita, N., Sato, B., Hirano, T., & Tamura, M. 2009, *PASJ*, 61, L35  
 Narita, N., et al. 2005, *PASJ*, 57, 471  
 Narita, N., et al. 2007, *PASJ*, 59, 763  
 Nettelmann, N., Fortney, J. J., Kramm, U., & Redmer, R. 2011, *ApJ*, 733, 2  
 Ogiwara, M., & Ida, S. 2009, *ApJ*, 699, 824  
 Ohta, Y., Taruya, A., & Suto, Y. 2009, *ApJ*, 690, 1  
 Press, W. H., Teukolsky, S. A., Vetterling, W. T., & Flannery, B. P. 1992, *Numerical recipes in C. The art of scientific computing* (Cambridge: University Press, —c1992, 2nd ed.)  
 Redfield, S., Endl, M., Cochran, W. D., & Koesterke, L. 2008, *ApJL*, 673, L87  
 Rogers, L. A., & Seager, S. 2010, *ApJ*, 716, 1208  
 Seager, S., & Sasselov, D. D. 2000, *ApJ*, 537, 916  
 Sing, D. K., et al. 2011, *MNRAS*, 416, 1443

- Snellen, I. A. G., Albrecht, S., de Mooij, E. J. W., & Le Poole, R. S. 2008, *A&A*, 487, 357
- Southworth, J. 2008, *MNRAS*, 386, 1644
- Swain, M. R., Vasisht, G., & Tinetti, G. 2008, *Nature*, 452, 329
- Tinetti, G., et al. 2007, *Nature*, 448, 169
- Triaud, A. H. M. J. 2011, *A&A*, 534, L6
- Valencia, D., Sasselov, D. D., & O'Connell, R. J. 2007, *ApJ*, 665, 1413
- Ward, W. R. 1986, *Icarus*, 67, 164
- Winn, J. N., Johnson, J. A., Albrecht, S., Howard, A. W., Marcy, G. W., Crossfield, I. J., & Holman, M. J. 2009, *ApJL*, 703, L99
- Winn, J. N., Suto, Y., Turner, E. L., Narita, N., Frye, B. L., Aoki, W., Sato, B., & Yamada, T. 2004, *PASJ*, 56, 655
- Winn, J. N., et al. 2005, *ApJ*, 631, 1215